 CMES, vol.46, no.3, pp.221-252, 2009

Boundary Reconstruction in Two-Dimensional Functionally Graded Materials Using a Regularized MFS

Liviu Marin[1]

Abstract: We investigate the stable numerical reconstruction of an unknown portion of the boundary of a two-dimensional domain occupied by a functionally graded material (FGM) from a given boundary condition on this part of the boundary and additional Cauchy data on the remaining known portion of the boundary. The aforementioned inverse geometric problem is approached using the method of fundamental solutions (MFS), in conjunction with the Tikhonov regularization method. The optimal value of the regularization parameter is chosen according to Hansen's L-curve criterion. Various examples are considered in order to show that the proposed method is numerically stable with respect to decreasing the amount of noise added into the Cauchy data, accurate and computationally very efficient.

Keywords: Functionally Graded Materials (FGMs); Inverse Geometric Problem; Method of Fundamental Solutions (MFS); Regularization.

1 Introduction

The method of fundamental solutions (MFS) is a meshless/meshfree boundary collocation method which is applicable to boundary value problems for which a fundamental solution of the operator in the governing equation is known. In spite of this restriction, it has, in recent years, become very popular primarily because of the ease with which it can be implemented, in particular for problems in complex geometries. Since its introduction as a numerical method by Mathon and Johnston (1977), it has been successfully applied to a large variety of physical problems, an account of which may be found in the survey papers [Fairweather and Karageorghis (1998); Golberg and Chen (1999); Fairweather, Karageorghis and Martin (2003); Cho, Golberg, Muleshkov and Li (2004)].

The ease of implementation of the MFS for problems with complex boundaries makes it an ideal candidate for problems in which the boundary is of major im-

[1] Institute of Solid Mechanics, Romanian Academy, 15 Constantin Mille, Sector 1, P.O. Box 1-863, 010141 Bucharest, Romania. E-mails: marin.liviu@gmail.com; liviu@imsar.bu.edu.ro

portance or requires special attention, such as inverse problems. For these reasons, the MFS has been used increasingly over the last decade for the numerical solution of the above class of problems. Recently, the MFS has been successfully applied to solving inverse problems associated with the heat equation [Hon and Wei (2004); Hon and Wei (2005); Mera (2005); Dong, Sun and Meng (2007); Ling and Takeuchi (2008); Marin (2008); Young, Tsai, Chen and Fan (2008); Shigeta and Young (2009)], linear elasticity [Marin and Lesnic (2004); Marin (2005a); Fam and Rashed (2009)], steady-state heat conduction in functionally graded materials (FGMs) [Marin (2005b)], Helmholtz-type equations [Marin (2005c); Marin and Lesnic (2005a); Jin and Zheng (2006)], Stokes problems [Chen, Young, Tsai and Murugesan (2005)], biharmonic equation [Marin and Lesnic (2005b); Zeb, Ingham and Lesnic (2008)], source reconstruction in heat conduction problems [Jin and Marin (2007); Yan, Fu and Yang (2008); Ahmadabadi, Arab and Ghaini (2009)], etc.

A classical example of an inverse problem in mechanics is the so-called *inverse geometric problem* . For such an inverse problem, both Dirichlet and Neumann data, i.e. Cauchy data, can be measured on an accessible and known part of the boundary of the solution domain, while either Dirichlet, or Neumann, or Robin-type condition is prescribed on the remaining, inaccessible and unknown part of the boundary. The goal is to reconstruct the unknown part of the boundary from the aforementioned available boundary conditions. There are several important studies in the literature devoted to the numerical solution of inverse geometric problems associated with various partial differential operators. Hsieh and Kassab (1986) proposed a general numerical method to determine an unknown boundary for heat conduction problems which is independent of the type of condition imposed on the unknown boundary. Huang and Chao (1997) investigated a steady-state shape identification problem by using both the Levenberg-Marquardt and the conjugate gradient methods. Their work was later extended by Huang and Tsai (1998) to a transient inverse geometric problem in identifying the irregular boundary configurations from external measurements using the boundary element method (BEM). Park and Ku (2001) considered the inverse problem of identifying the boundary shape of a domain from boundary temperature measurements, when the temperature is dominated by natural convection. Lesnic, Berger and Martin (2002) approached the boundary determination in potential corrosion damage from Cauchy data available on the known portion of the boundary by employing a regularized BEM minimization technique. Their method was also extended to the Lamé system of linear elasticity and Helmholtz-type equations both in two dimensions by Marin and Lesnic (2003), and Marin (2006), respectively.

The first attempt to solve an inverse geometric problem by a meshless method

was carried out in Hon and Wu (2000), where radial basis functions were used to approximate the solution. Apparently, the MFS was used for the first time in the solution of an inverse boundary determination problem in Mera and Lesnic (2005), where the authors solved the corresponding inverse problem associated with the three-dimensional Laplace equation arising in potential corrosion damage. Zeb, Ingham and Lesnic (2008) applied the MFS, without any physical constraints though, to the solution of an inverse boundary determination problem associated with the two-dimensional biharmonic equation. Hon and Li (2008) applied the MFS to solving one- and two-dimensional inverse boundary determination heat conduction problems. A combined MFS-Tikhonov regularization method was recently employed by Marin, Karageorghis and Lesnic (2009) to reconstruct, for two-dimensional harmonic problems, the inaccessible part of the boundary of the domain from Cauchy data on the remaining accessible portion of the boundary.

FGMs have recently been introduced and applied in the development of structural components subject to non-uniform service requirements. These materials possess continuously varying microstructure and mechanical and/or thermal properties. FGMs are essentially two-phase particulate composites, e.g. ceramic and metallic alloy phases, synthesized such that the composition of each constituent changes continuously in one direction, to yield a predetermined composition profile [Suresh and Mortensen (1998)]. Although the initial application of FGMs was to synthesize thermal barrier coatings for space applications, later investigations uncovered a wide variety of potential applications, such as nuclear fast breeder reactors, graded refractive index materials in audio-video disks, piezoelectric and thermoelectric devices, dental and medical implants, thermionic converters etc. However, for the sake of the physical explanation, we will refer in this study to the steady-state heat conduction problem for FGMs.

To our knowledge, inverse geometric problems in steady-state heat conduction in two-dimensional FGMs, have not, as yet, been investigated. Hence we address the following problem: In the framework of steady-state heat conduction in two-dimensional FGMs, determine in a stable manner the shape of an inaccessible and unknown part of the boundary of the solution domain, from a prescribed boundary condition on this portion of the boundary and Cauchy data available on the remaining, accessible and known part of the boundary. This inverse problem is approached using the MFS, in conjunction with the Tikhonov first-order regularization method [Tikhonov and Arsenin (1986)], while the optimal value of the regularization parameter is chosen according to Hansen's L-curve criterion [Hansen (1998)].

2 Mathematical formulation

Consider an open bounded domain $\Omega \subset \mathbb{R}^2$ occupied by an exponentially graded anisotropic solid and assume that Ω is bounded by a piecewise smooth curve $\partial\Omega$, such that $\partial\Omega = \partial\Omega_1 \cup \partial\Omega_2$, where $\partial\Omega_1 \neq \emptyset$, $\partial\Omega_2 \neq \emptyset$ and $\partial\Omega_1 \cap \partial\Omega_2 = \emptyset$. The thermal conductivities of this material can be expressed as, [Marin (2005b)]

$$\mathrm{k}_{ij}(\mathbf{x}) = \mathrm{K}_{ij} \exp(2\boldsymbol{\beta}\cdot\mathbf{x}), \quad \mathbf{x} = (\mathrm{x}_1, \mathrm{x}_2) \in \Omega, \quad i, j = 1, 2, \tag{1}$$

where the constant real or pure imaginary vector $\boldsymbol{\beta} = (\beta_1, \beta_2)$ characterizes the direction and the magnitude of the variation and the matrix $\mathbb{K} = [\mathrm{K}_{ij}]_{1\leq i,j\leq 2}$ is symmetric and positive-definite. It should be noted that $\mathbb{K} = [\delta_{ij}]_{1\leq i,j\leq 2}$ in the case of an isotropic material, where δ_{ij} is the Kronecker delta tensor. Then the heat flux in the solid is expressed as

$$\varphi_i(\mathbf{x}) = -\sum_{j=1}^{2} \mathrm{k}_{ij}(\mathbf{x})\partial_j \mathrm{u}(\mathbf{x}), \quad \mathbf{x} \in \Omega, \quad i = 1, 2, \tag{2}$$

where $\mathrm{u}(\mathbf{x})$ represents the temperature at $\mathbf{x} \in \Omega$ and $\partial_j \equiv \partial/\partial \mathrm{x}_j$. On using equations (1) and (2), the Fourier law in the absence of heat sources, namely,

$$\sum_{i=1}^{2} \partial_i \varphi_i(\mathbf{x}) = 0, \quad \mathbf{x} \in \Omega, \tag{3}$$

can be expressed in terms of the temperature, u, as

$$-\sum_{i,j=1}^{2} \Big(\mathrm{K}_{ij}\,\partial_i\partial_j \mathrm{u}(\mathbf{x}) + 2\beta_i \mathrm{K}_{ij}\,\partial_j \mathrm{u}(\mathbf{x}) \Big) \exp(2\boldsymbol{\beta}\cdot\mathbf{x}) = 0, \quad \mathbf{x} \in \Omega. \tag{4}$$

We now let $\mathbf{n}(\mathbf{x})$ be the unit outward normal vector at $\partial\Omega$ and $\mathrm{q}(\mathbf{x})$ be the normal heat flux at a point $\mathbf{x} \in \partial\Omega$ defined by

$$\mathrm{q}(\mathbf{x}) = \sum_{i=1}^{2} \mathrm{n}_i(\mathbf{x})\varphi_i(\mathbf{x}) = -\sum_{i,j=1}^{2} \mathrm{n}_i(\mathbf{x})\mathrm{k}_{ij}(\mathbf{x})\partial_j \mathrm{u}(\mathbf{x}), \quad \mathbf{x} \in \partial\Omega. \tag{5}$$

In the direct problem formulation, the knowledge of the thermal conductivity matrix $\mathbb{K}$, the vector $\boldsymbol{\beta}$, the location, shape and size of the entire boundary $\partial\Omega$, the

temperature and/or normal heat flux on the entire boundary $\partial\Omega$ gives the corresponding Dirichlet, Neumann, or Robin conditions which enable us to determine the unknown boundary conditions, as well as the temperature distribution in the solution domain. A different and more interesting situation occurs when a part of the boundary is unknown, say $\partial\Omega_2$, whilst some additional information is supplied on the remaining part of the boundary $\partial\Omega_1 = \partial\Omega \setminus \partial\Omega_2$. More precisely, we consider the following inverse geometric problem for two-dimensional FGMs:

Determine the boundary $\partial\Omega_2 \subset \partial\Omega$, $\partial\Omega_2 \neq \emptyset$, such that the temperature u satisfies the Fourier law (3), or its equivalent form (4), both temperature and flux conditions, i.e. Cauchy data, are given on the known part of the boundary, and either Dirichlet, or Neumann, or Robin boundary condition is prescribed on $\partial\Omega_2$, namely

$$-\sum_{i,j=1}^{2}\Big(\mathrm{K}_{ij}\,\partial_i\partial_j \mathrm{u}(\mathbf{x}) + 2\beta_i\,\mathrm{K}_{ij}\,\partial_j \mathrm{u}(\mathbf{x})\Big)\exp\left(2\boldsymbol{\beta}\cdot\mathbf{x}\right) = 0, \quad \mathbf{x}\in\Omega, \tag{6a}$$

$$\mathrm{u}(\mathbf{x}) = \widetilde{\mathrm{u}}(\mathbf{x}), \quad \mathbf{x}\in\partial\Omega_1, \tag{6b}$$

$$\mathrm{q}(\mathbf{x}) = \widetilde{\mathrm{q}}(\mathbf{x}), \quad \mathbf{x}\in\partial\Omega_1, \tag{6c}$$

$$\alpha_{\mathrm{u}}\,\mathrm{u}(\mathbf{x}) + \alpha_{\mathrm{q}}\,\mathrm{q}(\mathbf{x}) = \widetilde{\mathrm{f}}(\mathbf{x}), \quad \mathbf{x}\in\partial\Omega_2, \tag{6d}$$

where $\alpha_{\mathrm{u}}, \alpha_{\mathrm{q}} \in \mathbb{R}$, while $\widetilde{\mathrm{u}}$, $\widetilde{\mathrm{q}}$ and $\widetilde{\mathrm{f}}$ are prescribed Dirichlet, Neumann and Robin boundary conditions, respectively. It should be noted that, in Eq. $(6d)$, the cases when $\alpha_{\mathrm{u}} = 1$ and $\alpha_{\mathrm{q}} = 0$, and $\alpha_{\mathrm{u}} = 0$ and $\alpha_{\mathrm{q}} = 1$ correspond to given Dirichlet and Neumann boundary conditions on $\partial\Omega_2$, respectively, whilst the condition $\alpha_{\mathrm{u}}\,\alpha_{\mathrm{q}} \neq 0$ is associated with prescribed Robin boundary condition on $\partial\Omega_2$.

In addition, we also assume that the known boundary $\partial\Omega_1$ is the graph of a known Lipschitz function $\phi_1 : [-r,r] \longrightarrow [0,\infty)$, whilst the unknown boundary $\partial\Omega_2$ is the graph of an unknown Lipschitz function $\phi_2 : [-r,r] \longrightarrow \mathbb{R}$, where $\phi_1(\mathrm{x}) > \phi_2(\mathrm{x})$ for all $\mathrm{x} \in (-r,r)$. Moreover, both the known and unknown boundaries intersect the x_1-coordiante axis at the points $(\pm r, 0)$, see e.g. Fig. 1.

This inverse geometric problem is much more difficult to solve both analytically and numerically than the direct problem, since the solution does not satisfy the general conditions of well-posedness. Although the problem may have a unique solution, it is well known, see e.g. Hadamard (1923), that this solution is unstable with respect to small perturbations in the data on $\partial\Omega_1$. Thus the problem is ill-posed and we cannot use a direct approach to solve it in a stable manner.

3 Method of fundamental solutions

3.1 Boundary discretization

The boundary $\partial\Omega$ of the solution domain Ω is discretized by selecting the N_1 boundary points $\mathbf{z}^{(i)}$, $i=1,\ldots,N_1$, on the known boundary $\partial\Omega_1$ and the N_2 boundary points $\mathbf{z}^{(N_1+i)}$, $i=1,\ldots,N_2$, on the unknown boundary $\partial\Omega_2$, such that $N=N_1+N_2$. Consequently, the boundary $\partial\Omega$ is approximated by

$$\partial\Omega \approx \partial\widetilde{\Omega} = \bigcup_{i=1}^{N_1+N_2} \Gamma^{(i)}, \quad \text{where} \quad \Gamma^{(i)} = \left[\mathbf{z}^{(i)}, \mathbf{z}^{(i+1)}\right], \quad i=1,\ldots,N_1+N_2, \tag{7}$$

with the following convention $\mathbf{z}^{(N_1+N_2+1)} = \mathbf{z}^{(1)}$. Note that as a direct consequence of the discretization given by Eq. (7), the known and unknown boundaries $\partial\Omega_1$ and $\partial\Omega_2$, respectively, are approximated by

$$\partial\Omega_1 \approx \partial\widetilde{\Omega}_1 = \bigcup_{i=1}^{N_1} \Gamma^{(i)} \quad \text{and} \quad \partial\Omega_2 \approx \partial\widetilde{\Omega}_2 = \bigcup_{i=N_1+1}^{N_1+N_2} \Gamma^{(i)}. \tag{8}$$

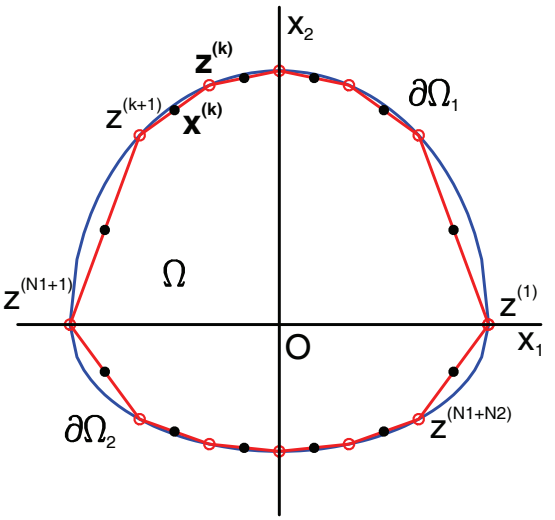

Figure 1: Geometry and boundary discretization of the problem.

Further, we consider the MFS boundary collocation points to be the midpoints $\mathbf{x}^{(i)}$, $i=1,\ldots,N_1+N_2$, of each segment $\Gamma^{(i)}$, $i=1,\ldots,N_1+N_2$, namely

$$\mathbf{x}^{(i)} = \frac{1}{2}\left(\mathbf{z}^{(i)} + \mathbf{z}^{(i+1)}\right) = \mathbf{x}^{(i)}\left(\mathbf{z}^{(i)}, \mathbf{z}^{(i+1)}\right), \quad i = 1, \ldots, N_1 + N_2. \tag{9}$$

In this way, the outward unit normal vector $\mathbf{n}$ to the approximate boundary $\partial\widetilde{\Omega}$ at the MFS boundary collocation points is given by

$$\mathbf{n}(\mathbf{x}^{(i)}) = \frac{1}{\|\mathbf{z}^{(i+1)} - \mathbf{z}^{(i)}\|}\left(\mathrm{z}_2^{(i+1)} - \mathrm{z}_2^{(i)}, -\mathrm{z}_1^{(i+1)} + \mathrm{z}_1^{(i)}\right), \quad i = 1, \ldots, N_1 + N_2. \tag{10}$$

In this study, the boundary points $\mathbf{z}^{(i)}$, $i = 1, \ldots, N_1 + N_2$, are chosen such that their x_1-components are uniformly distributed on the segment $[-r, r]$, while the x_2-components are expressed as functions of the corresponding x_1-components. More specifically, with respect to Fig. 1, we have

$$\mathbf{z}^{(i)} = \left(\mathrm{z}_1^{(i)}, \mathrm{z}_2^{(i)}\right), \quad i = 1, \ldots, N_1 + N_2, \tag{11a}$$

$$\mathrm{z}_1^{(i)} = r\left(1 - 2\frac{i-1}{N_1}\right), \quad \mathrm{z}_2^{(i)} = \phi_1(\mathrm{z}_1^{(i)}), \quad i = 1, \ldots, N_1, \tag{11b}$$

$$\mathrm{z}_1^{(N_1+i)} = -r\left(1 - 2\frac{i-1}{N_2}\right), \quad \mathrm{z}_2^{(N_1+i)} = \phi_2(\mathrm{z}_1^{(N_1+i)}), \quad i = 1, \ldots, N_2, \tag{11c}$$

$$\mathbf{z}^{(1)} = (r, 0), \quad \mathbf{z}^{(N_1+1)} = (-r, 0). \tag{11d}$$

Hence from Eqs. (9) and (11), it follows that the unknown boundary $\partial\Omega_2$ is completely determined by the unknown vector $\mathbf{z} = \left[\mathrm{z}_2^{(N_1+2)}, \ldots, \mathrm{z}_2^{(N_1+N_2)}\right]^{\mathsf{T}} \in \mathbb{R}^{N_2-1}$.

3.2 MFS approximation

The fundamental solution G of the heat balance equation (3), or equivalently (4), for two-dimensional anisotropic FGMs is given by [Marin (2005b)]

$$G(\mathbf{x}, \boldsymbol{\xi}) = -\frac{K_0(\kappa \mathrm{R})}{2\pi\sqrt{\det \mathbb{K}}} \exp\{-\boldsymbol{\beta} \cdot (\mathbf{x} + \boldsymbol{\xi})\}, \quad \mathbf{x} \in \overline{\Omega}, \quad \boldsymbol{\xi} \in \mathbb{R}^2 \setminus \overline{\Omega}, \tag{12}$$

where $\boldsymbol{\xi}$ is a singularity or source point, K_0 is the modified Bessel function of the second kind of order zero, $\kappa = \sqrt{\boldsymbol{\beta} \cdot \mathbb{K}\boldsymbol{\beta}}$, $\mathrm{R} = \sqrt{\mathbf{r} \cdot \mathbb{K}^{-1}\mathbf{r}}$ and $\mathbf{r} = \mathbf{x} - \boldsymbol{\xi}$.

The main idea of the MFS consists of the approximation of the temperature in the solution domain by a linear combination of fundamental solutions with respect to M singularities $\boldsymbol{\xi}^{(j)}$, $j = 1,\ldots,M$, in the form

$$\mathrm{u}(\mathbf{x}) \approx \mathrm{u}_M(\mathbf{c},\boldsymbol{\xi};\mathbf{x}) = \sum_{j=1}^{M} \mathrm{c}_j\, G(\mathbf{x},\boldsymbol{\xi}^{(j)}), \quad \mathbf{x} \in \overline{\Omega}, \tag{13}$$

where $\mathbf{c} = [\mathrm{c}_1,\ldots,\mathrm{c}_M]^{\mathsf{T}}$ and $\boldsymbol{\xi} \in \mathbb{R}^{2M}$ is a vector containing the coordinates of the singularities $\boldsymbol{\xi}^{(j)}$, $j = 1,\ldots,M$. On taking into account the definitions of the heat flux (2), the normal heat flux (5) and the fundamental solution (12) then the normal heat flux, through a curve defined by the outward unit normal vector $\mathbf{n}(\mathbf{x})$, can be approximated on the boundary $\partial\Omega$ by

$$\mathrm{q}(\mathbf{x}) \approx \mathrm{q}_M(\mathbf{c},\boldsymbol{\xi};\mathbf{x}) = \sum_{j=1}^{M} \mathrm{c}_j\, H(\mathbf{x},\boldsymbol{\xi}^{(j)}), \quad \mathbf{x} \in \partial\Omega, \tag{14}$$

where

$$\begin{aligned} H(\mathbf{x},\boldsymbol{\xi}) &= -\sum_{i,j=1}^{2} \mathrm{n}_i(\mathbf{x})\, \mathrm{K}_{ij}\, \partial_j G(\mathbf{x},\boldsymbol{\xi}) \exp(2\boldsymbol{\beta}\cdot\mathbf{x}) \\ &= -\frac{\exp(\boldsymbol{\beta}\cdot\mathbf{r})}{2\pi\sqrt{\det\mathbb{K}}} \left[\frac{\kappa}{\mathrm{R}} (\mathbf{n}(\mathbf{x})\cdot\mathbf{r})\, K_1(\kappa\mathrm{R}) + (\mathbf{n}(\mathbf{x})\cdot\mathbb{K}\boldsymbol{\beta})\, K_0(\kappa\mathrm{R})\right], \\ &\mathbf{x} \in \partial\Omega, \quad \boldsymbol{\xi} \in \mathbb{R}^2 \setminus \overline{\Omega}, \end{aligned} \tag{15}$$

with K_1 the modified Bessel function of second kind of order one.

According to the MFS approximations (13) and (14), the discretized version of the boundary conditions $(6b)-(6d)$ recasts as

$$\sum_{j=1}^{M} G(\mathbf{x}^{(i)},\boldsymbol{\xi}^{(j)})\, \mathrm{c}_j = \widetilde{\mathrm{u}}(\mathbf{x}^{(i)}), \quad i = 1,\ldots,N_1, \tag{16a}$$

$$\sum_{j=1}^{M} H(\mathbf{x}^{(i)},\boldsymbol{\xi}^{(j)})\, \mathrm{c}_j = \widetilde{\mathrm{q}}(\mathbf{x}^{(i)}), \quad i = 1,\ldots,N_1, \tag{16b}$$

$$\sum_{j=1}^{M}\left[\alpha_{\mathrm{u}}\,G(\mathbf{x}^{(i)},\boldsymbol{\xi}^{(j)})+\alpha_{\mathrm{q}}\,H(\mathbf{x}^{(i)},\boldsymbol{\xi}^{(j)})\right]\mathrm{c}_j=\widetilde{\mathrm{f}}(\mathbf{x}^{(i)}),\quad i=N_1+1,\ldots,N_1+N_2. \tag{16c}$$

Eqs. $(16a)-(16c)$ represent a system of $2N_1+N_2$ nonlinear algebraic equations with $M+N_2-1$ unknowns, namely the MFS coefficients $\mathbf{c}=[\mathrm{c}_1,\ldots,\mathrm{c}_M]^{\mathsf{T}}\in\mathbb{R}^M$ and the x_2-coordinates $\mathbf{z}=\left[\mathrm{z}_2^{(N_1+2)},\ldots,\mathrm{z}_2^{(N_1+N_2)}\right]^{\mathsf{T}}\in\mathbb{R}^{N_2-1}$ of the boundary points that determine the unknown boundary $\partial\Omega_2$. It should be noted that in order to uniquely determine the solution $(\mathbf{c},\mathbf{z})\in\mathbb{R}^M\times\mathbb{R}^{N_2-1}$ of the system of nonlinear algebraic equations $(16a)-(16c)$, the number N_1 of MFS boundary collocation points on the known boundary $\partial\Omega_1$ and the number M of singularities must satisfy the inequality $M-1\leq 2N_1$. However, the system of nonlinear algebraic equations $(16a)-(16c)$ cannot be solved by direct methods, such as the least-squares method, since such an approach would produce a highly unstable solution.

3.3 MFS boundary collocation points and singularities

In order to implement the MFS, the location of the singularities has to be determined and this is usually achieved by considering either the static or the dynamic approach. In the static approach, the singularities are pre-assigned and kept fixed throughout the solution process, while in the dynamic approach, the singularities and the unknown coefficients are determined simultaneously during the solution process, see Fairweather and Karageorghis (1998). For nonlinear systems, the uniqueness of the solution is not always guaranteed and it is computationally much more expensive. Thus the dynamic approach transforms the inverse geometric problem into a more difficult nonlinear ill-posed problem. Therefore, we have decided to employ the static approach in our computations with the singularities, $\boldsymbol{\xi}^{(j)}$, $j=1,\ldots,M$, located on the boundary, $\partial\Omega_S$, of the disk of radius R_S and centered at the origin, $\Omega_S=\left\{\mathbf{x}=(\mathrm{x}_1,\mathrm{x}_2)\,\middle|\,\mathrm{x}_1^2+\mathrm{x}_2^2<\mathrm{R}_S^2\right\}$, with the mention that R_S is taken sufficiently large such that $\overline{\Omega}\subset\Omega_S$.

Although not considered herein, it should be mentioned that the dynamic approach for selecting the location of the MFS singularities can also be adopted. In this case, two situations can occur:

(i) The singularities, $\boldsymbol{\xi}^{(j)}$, $j=1,\ldots,M$, are located on the boundary $\partial\Omega_S$ of the disk $\Omega_S=\left\{\mathbf{x}=(\mathrm{x}_1,\mathrm{x}_2)\,\middle|\,\mathrm{x}_1^2+\mathrm{x}_2^2<\mathrm{R}_S^2\right\}$ and hence the radius R_S also becomes an unknown of the problem.

(ii) The singularities, $\boldsymbol{\xi}^{(j)}$, $j=1,\ldots,M$, are located on the pseudo-boundary $\partial\Omega_S$, which has the same shape as the boundary $\partial\Omega$ and is situated at a distance $d>0$ from $\partial\Omega$ such that $\overline{\Omega}\subset\Omega_S$, and hence the distance d also becomes an unknown of the problem.

4 Description of the algorithm

In this section, we present a numerical scheme for the stable solution of the system of nonlinear algebraic equations $(16a)-(16c)$, as well as details regarding the numerical implementation of the proposed method.

4.1 Tikhonov regularization method

Several regularization techniques used for solving stably systems of linear and nonlinear algebraic equations are available in the literature, such as the Singular Value Decomposition (SVD) [Hansen (1998)], Tikhonov regularization method [Tikhonov and Arsenin (1986)] and iterative methods [Kunisch and Zou (1998)]. Recently, Liu (2008a) proposed a new and robust numerical technique for the stable solution of ill-posed systems of linear algebraic equations, namely the Fictitious Time Integration Method (FTIM). The FTIM consists of introducing a fictitious time that plays the role of a regularization parameter, while its filtering effect being better than that of the Tikhonov and exponential filters. This method was successfully used for solving inverse vibration problems [Liu (2008b); Liu (2008c); Liu, Chang, Chang and Chen (2008)], nonlinear complementarity problems [Liu (2008d)], boundary value problems for elliptic partial differential equations [Liu (2008e)], m-point boundary value problems for ordinary differential equations [Liu (2008f)], mixed-complementarity problems and optimization problems [Liu and Atluri (2008a)] and inverse Sturm-Liouville problems [Liu and Atluri (2008b)]. Liu and Atluri (2009) have recently shown that, when applied to solving an ill-posed system of linear equations, the general FTIM may be interpreted as leading, as a special case, to the Tiknonov regularization method.

However, the inverse geometric problem investigated in this paper is solved, in a stable manner, by minimizing the following Tikhonov regularization functional, see Tikhonov and Arsenin (1986)

$$\mathscr{F}_\lambda(\cdot,\cdot):\mathbb{R}^M\times\mathbb{R}^{N_2-1}\longrightarrow[0,\infty),\quad \mathscr{F}_\lambda(\mathbf{c},\mathbf{z})=\mathscr{F}_{LS}(\mathbf{c},\mathbf{z})+\mathscr{R}_\lambda(\mathbf{z}), \tag{17}$$

where $\mathscr{F}_{LS}$ is the least-squares functional associated with the inverse geometric problem investigated in this study, $\mathscr{R}_\lambda$ is the regularization term to be specified and $\lambda>0$ is the regularization parameter to be prescribed.

The least-squares functional, $\mathscr{F}_{LS}$, in Eq. (17) given by

$$\begin{aligned}
&\mathscr{F}_{LS}(\cdot,\cdot) : \mathbb{R}^{M} \times \mathbb{R}^{N_2-1} \longrightarrow [0,\infty),\\
&\mathscr{F}_{LS}(\mathbf{c},\mathbf{z}) = \frac{1}{2}\sum_{i=1}^{N_1}\left\{\left[\mathscr{F}_1(\mathbf{c},\boldsymbol{\xi};\mathbf{x}^{(i)})\right]^2 + \left[\mathscr{F}_2(\mathbf{c},\boldsymbol{\xi};\mathbf{x}^{(i)})\right]^2\right\}\\
&+\frac{1}{2}\sum_{i=N_1+1}^{N_1+N_2}\left[\mathscr{F}_3(\mathbf{c},\boldsymbol{\xi};\mathbf{x}^{(i)})\right]^2,
\end{aligned} \tag{18}$$

where

$$\mathscr{F}_1(\mathbf{c},\boldsymbol{\xi};\mathbf{x}^{(i)}) = \widetilde{\mathrm{u}}(\mathbf{x}^{(i)}) - \mathrm{u}_M(\mathbf{c},\boldsymbol{\xi};\mathbf{x}^{(i)}), \quad i = 1,\ldots,N_1, \tag{19a}$$

$$\mathscr{F}_2(\mathbf{c},\boldsymbol{\xi};\mathbf{x}^{(i)}) = \widetilde{\mathrm{q}}(\mathbf{x}^{(i)}) - \mathrm{q}_M(\mathbf{c},\boldsymbol{\xi};\mathbf{x}^{(i)}), \quad i = 1,\ldots,N_1, \tag{19b}$$

$$\begin{aligned}
&\mathscr{F}_3(\mathbf{c},\boldsymbol{\xi};\mathbf{x}^{(i)}) = \widetilde{\mathrm{f}}(\mathbf{x}^{(i)}) - \left[\alpha_{\mathrm{u}}\,\mathrm{u}_M(\mathbf{c},\boldsymbol{\xi};\mathbf{x}^{(i)}) + \alpha_{\mathrm{q}}\,\mathrm{q}_M(\mathbf{c},\boldsymbol{\xi};\mathbf{x}^{(i)})\right],\\
&i = N_1+1,\ldots N_1+N_2.
\end{aligned} \tag{19c}$$

In this paper, the regularization term, $\mathscr{R}_\lambda$, in Eq. (17) was chosen to be the Tikhonov first-order regularization term, namely

$$\mathscr{R}_\lambda(\cdot) : \mathbb{R}^{N_2-1} \longrightarrow [0,\infty), \quad \mathscr{R}_\lambda(\mathbf{z}) = \lambda\,\|\mathbf{z}'\|^2. \tag{20}$$

Here $\mathbf{z}' = \left[\mathrm{z}_2^{(N_1+2)} - \mathrm{z}_2^{(N_1+1)}, \ldots, \mathrm{z}_2^{(N_1+N_2+1)} - \mathrm{z}_2^{(N_1+N_2)}\right]^{\mathsf{T}}$ denotes an approximation to the first order derivative to the function ϕ_2, keeping in mind that $\mathrm{z}_1^{(i+1)} - \mathrm{z}_1^{(i)}$, $i = N_1,\ldots,N_1+N_2$, is constant.

It should be emphasized that the zeroth-order Tikhonov regularization procedure, which is based on penalizing the norm of the solution, i.e. $\mathscr{R}_\lambda(\mathbf{z}) = \lambda\|\mathbf{z}\|^2$ in Eq. (17), rather than its derivative, i.e. $\mathscr{R}_\lambda(\mathbf{z}) = \lambda\|\mathbf{z}'\|^2$ as given Eq. (17), did not produce satisfactorily accurate and stable results for the unknown boundary $\partial\Omega_2$. This observation is consistent with the results obtained by Peneau, Jarny and Sarda (1996), Lesnic, Berger and Martin (2002), and Marin, Karageorghis and Lesnic (2009); Marin and Lesnic (2003); and Marin (2006) who have solved a similar problem for the Laplace equation, the Lamé system and Helmholtz-type equations, respectively. However, Zeb, Ingham and Lesnic (2008) successfully employed the zeroth-order Tikhonov regularization functional, without imposing any physical constraints on the x_2-coordinates of the unknown boundary $\partial\Omega_2$.

4.2 Physical constraints

In order to retrieve an accurate and physically correct numerical solution of the inverse geometric problem investigated herein, the Tikhonov first-order functional given by Eq. (17) is minimized subject to the following simple bounds imposed for the components of the unknown vector $\mathbf{z} = \left[z_2^{(N_1+2)}, \ldots, z_2^{(N_1+N_2)} \right]^{\mathsf{T}} \in \mathbb{R}^{N_2-1}$:

$$-\sqrt{R_S^2 - \left(z_1^{(i)}\right)^2} < z_2^{(i)} < \phi_1(z_2^{(i)}), \quad i = N_1+2, \ldots, N_1+N_2. \tag{21}$$

The simple bounds (21) require that the x_2-coordinates of the unknown boundary $\partial\Omega_2$ are situated below those corresponding to the known boundary $\partial\Omega_2$, while, at the same time, the singularities are located outside $\overline{\Omega}$. Alternatively, one can impose different lower and/or upper bounds for the components of the unknown vector $\mathbf{z} \in \mathbb{R}^{N_2-1}$, provided that some additional *a priori* information about the location of the unknown boundary $\partial\Omega_2$ is known. For example, if it is known that the x_2-coordinates of the unknown boundary $\partial\Omega_2$ are situated below the x_1-axis then the simple bounds (21) can be replaced with the following ones:

$$-\sqrt{R_S^2 - \left(z_1^{(i)}\right)^2} < z_2^{(i)} < 0, \quad i = N_1+2, \ldots, N_1+N_2. \tag{22}$$

To summarize, the Tikhonov regularization method solves a physically constrained minimization problem using a smoothness norm in order to provide a stable solution which fits the data and also has a minimum structure. More precisely, the MFS system of nonlinear algebraic equations $(16a)-(16c)$ associated with the inverse geometric problem given by Eqs. $(6a)-(6d)$ is solved numerically by minimizing the Tikhonov first-order regularization functional (17) with respect to the unknown $(\mathbf{c}, \mathbf{z}) \in \mathbb{R}^M \times \mathbb{R}^{N_2-1}$, subject to the physical constraints (21) or (22), i.e.

$$(\mathbf{c}_\lambda, \mathbf{z}_\lambda) : \mathscr{F}_\lambda(\mathbf{c}_\lambda, \mathbf{z}_\lambda) = \min_{(\mathbf{c},\mathbf{z}) \in \mathbb{R}^M \times \mathbb{R}^{N_2-1}} \left\{ \mathscr{F}_\lambda(\mathbf{c}, \mathbf{z}) \,\middle|\, \mathbf{z} \text{ satisfies (21) or (22)} \right\}. \tag{23}$$

4.3 Numerical implementation

The minimization of the constrained Tikhonov first-order regularization functional (23) is obtained using the NAG subroutine `E04UNF` [NAG Library Mark 21 (2007)] which minimizes a sum of squares subject to constraints. This may include simple bounds, linear constraints and smooth nonlinear constraints. Each iteration of the

subroutine E04UNF includes the following: (i) the solution of a quadratic programming subproblem; (ii) a line search with an augmented Lagrangian function; and (iii) a quasi-Newton update of the approximate Hessian of the Lagrangian function, see e.g. Gill, Murray and Wright (1981).

4.3.1 Tikhonov regularization functional

To implement a code using E04UNF, we firstly denote by $\boldsymbol{\eta} = (\mathbf{c}, \mathbf{z}) \in \mathbb{R}^{M+N_2-1}$ the vector containing the unknowns of the MFS system of nonlinear algebraic equations $(16a) - (16c)$ associated with the inverse geometric problem for two-dimensional FGMs given by Eqs. $(6a) - (6d)$, i.e.

$$\begin{aligned} &\eta_\ell = \mathrm{c}_\ell, && \ell = 1, \ldots, M, \\ &\eta_{M+\ell} = \mathrm{z}_2^{(N_1+\ell+1)}, && \ell = 1, \ldots, N_2 - 1. \end{aligned} \tag{24}$$

Then we re-write the Tikhonov first-order regularization functional defined by Eq. (17) in the following form:

$$\begin{aligned} &\mathscr{F}_\lambda(\cdot) : \mathbb{R}^{M+N_2-1} \longrightarrow [0, \infty), \\ &\mathscr{F}_\lambda(\boldsymbol{\eta}) = \underbrace{\frac{1}{2} \sum_{i=1}^{2N_1+N_2} \left[\overline{\mathrm{y}}_k - \overline{\mathrm{F}}_k(\boldsymbol{\eta})\right]^2}_{= \mathscr{F}_{LS}(\mathbf{c}, \mathbf{z})} + \underbrace{\frac{1}{2} \left[\overline{\mathrm{y}}_{2N_1+N_2+1} - \overline{\mathrm{F}}_{2N_1+N_2+1}(\boldsymbol{\eta})\right]^2}_{= \mathscr{R}_\lambda(\mathbf{z})}, \end{aligned} \tag{25}$$

where the vectors $\overline{\mathbf{F}}(\boldsymbol{\eta}) = \left[\overline{\mathrm{F}}_1(\boldsymbol{\eta}), \ldots, \overline{\mathrm{F}}_{2N_1+N_2+1}(\boldsymbol{\eta})\right]^{\mathsf{T}} \in \mathbb{R}^{2N_1+N_2-1}$ and $\overline{\mathbf{y}} = \left[\overline{\mathrm{y}}_1, \ldots, \overline{\mathrm{y}}_{2N_1+N_2+1}\right]^{\mathsf{T}} \in \mathbb{R}^{2N_1+N_2-1}$ are given by

$$\overline{\mathrm{F}}_k(\boldsymbol{\eta}) = \sum_{j=1}^{M} G(\mathbf{x}^{(k)}, \boldsymbol{\xi}^{(j)})\, \mathrm{c}_j, \quad \overline{\mathrm{y}}_k = \widetilde{\mathrm{u}}(\mathbf{x}^{(k)}), \quad k = 1, \ldots, N_1, \tag{26a}$$

$$\overline{\mathrm{F}}_{N_1+k}(\boldsymbol{\eta}) = \sum_{j=1}^{M} H(\mathbf{x}^{(k)}, \boldsymbol{\xi}^{(j)})\, \mathrm{c}_j, \quad \overline{\mathrm{y}}_{N_1+k} = \widetilde{\mathrm{q}}(\mathbf{x}^{(k)}), \quad k = 1, \ldots, N_1, \tag{26b}$$

$$\begin{aligned} &\overline{\mathrm{F}}_{2N_1+k}(\boldsymbol{\eta}) = \sum_{j=1}^{M} \left[\alpha_{\mathrm{u}}\, G(\mathbf{x}^{(k)}, \boldsymbol{\xi}^{(j)}) + \alpha_{\mathrm{q}}\, H(\mathbf{x}^{(k)}, \boldsymbol{\xi}^{(j)})\right] \mathrm{c}_j, \\ &\overline{\mathrm{y}}_{2N_1+k} = \widetilde{\mathrm{f}}(\mathbf{x}^{(k)}), \quad k = 1, \ldots, N_2, \end{aligned} \tag{26c}$$

$$\overline{\mathrm{F}}_{2N_1+N_2+1}(\boldsymbol{\eta}) = \sqrt{2\lambda}\left[\sum_{j=2}^{N_2+1}\left(\mathrm{z}_2^{(N_1+j)} - \mathrm{z}_2^{(N_1+j-1)}\right)^2\right]^{1/2}, \quad \overline{\mathrm{y}}_{2N_1+N_2+1} = 0. \tag{26d}$$

4.3.2 Gradient of the Tikhonov regularization functional

We define the components of the gradient, $\mathbf{J}(\boldsymbol{\eta}) = \nabla\mathscr{F}_\lambda(\boldsymbol{\eta}) \in \mathbb{R}^{(2N_1+N_2+1)\times(M+N_2-1)}$, corresponding to the Tikhonov first-order regularization functional, as defined in Eq. (25), by

$$\mathrm{J}_{k,\ell}(\boldsymbol{\eta}) = \begin{cases} G(\mathbf{x}^{(k)}, \boldsymbol{\xi}^{(\ell)}), & k = 1,\ldots,N_1, \quad \ell = 1,\ldots,M, \\ 0, & k = 1,\ldots,N_1, \quad \ell = M+1,\ldots,M+N_2-1, \end{cases} \tag{27a}$$

$$\mathrm{J}_{N_1+k,\ell}(\boldsymbol{\eta}) = \begin{cases} H(\mathbf{x}^{(k)}, \boldsymbol{\xi}^{(\ell)}), & k = 1,\ldots,N_1, \quad \ell = 1,\ldots,M, \\ 0, & k = 1,\ldots,N_1, \quad \ell = M+1,\ldots,M+N_2-1, \end{cases} \tag{27b}$$

$$\mathrm{J}_{2N_1+k,\ell}(\boldsymbol{\eta}) = \begin{cases} \alpha_{\mathrm{u}}\, G(\mathbf{x}^{(N_1+k)}, \boldsymbol{\xi}^{(\ell)}) + \alpha_{\mathrm{q}}\, H(\mathbf{x}^{(N_1+k)}, \boldsymbol{\xi}^{(\ell)}), \\ \qquad k = 1,\ldots,N_2, \quad \ell = 1,\ldots,M, \\ \displaystyle\sum_{j=1}^{M} \frac{\partial}{\partial\eta_\ell}\left[\alpha_{\mathrm{u}}\, G(\mathbf{x}^{(N_1+k)}, \boldsymbol{\xi}^{(j)}) + \alpha_{\mathrm{q}}\, H(\mathbf{x}^{(N_1+k)}, \boldsymbol{\xi}^{(j)})\right] \mathrm{c}_j, \\ \qquad k = 1,\ldots,N_2, \quad \ell = M+1,\ldots,M+N_2-1, \end{cases} \tag{27c}$$

$$\mathrm{J}_{2N_1+N_2+1,\ell}(\boldsymbol{\eta}) = \begin{cases} 0, & \ell = 1,\ldots,M, \\ \sqrt{2\lambda}\, \dfrac{\partial}{\partial\eta_\ell}\|\mathbf{z}'\|, & \ell = M+1,\ldots,M+N_2-1. \end{cases} \tag{27d}$$

It should be mentioned that providing as many exact value for the components of the gradient $\mathbf{J}(\boldsymbol{\eta}) = \nabla\mathscr{F}_\lambda(\boldsymbol{\eta})$ as possible to the NAG subroutine `E04UNF` results not only in an improvement in the accuracy of the numerical approximation of the unknown boundary, but also in a marked decrease in the computational time required to minimize the Tikhonov first-order regularization functional given by (17) with respect to the unknown vector $\boldsymbol{\eta} \in \mathbb{R}^{M+N_2-1}$, subject to the physical constraints (21) or (22).

4.3.3 Stability estimate

It is important to mention that if the right-hand side of Eqs. $(16a)-(16c)$ is corrupted by noise, i.e.

$$\|\mathbf{y}-\mathbf{y}^{\varepsilon}\| \leq \varepsilon, \tag{28}$$

where $\mathbf{y}^{\varepsilon} \in \mathbb{R}^{2N_1+N_2}$ is a perturbation of the vector $\mathbf{y} = \left[\overline{\mathrm{y}}_1, \ldots, \overline{\mathrm{y}}_{2N_1+N_2}\right]^{\mathsf{T}} \in \mathbb{R}^{2N_1+N_2}$ defined by Eqs. $(26a)-(26c)$, then the following stability estimate holds, see Engl, Hanke and Neubauer (2000),

$$\|\boldsymbol{\eta}_{\lambda}-\boldsymbol{\eta}_{\lambda}^{\varepsilon}\| \leq \frac{\varepsilon}{\lambda}, \tag{29}$$

where $\boldsymbol{\eta}_{\lambda} = (\mathbf{c}_{\lambda}, \mathbf{z}_{\lambda})$ and $\boldsymbol{\eta}_{\lambda}^{\varepsilon} = \left(\mathbf{c}_{\lambda}^{\varepsilon}, \mathbf{z}_{\lambda}^{\varepsilon}\right)$ are the numerical solutions to the constrained minimization problem (23) with exact and noisy right-hand sides, respectively.

5 Numerical results and discussion

It is the purpose of this section to present the performance of the proposed numerical method, namely the regularized MFS described in Section 4. To do so, we solve numerically the inverse geometric problem given by Eqs. $(6a)-(6d)$ for a two-dimensional FGM with $\mathrm{K}_{11} = 1.0$, $\mathrm{K}_{12} = \mathrm{K}_{12} = 0$, $\mathrm{K}_{22} = 1.0$, $\beta_1 = -0.5$ and $\beta_2 = 0.3$, in the two-dimensional geometries which are schematically presented in Figs. 2(a)–(d).

5.1 Examples

For all examples investigated in this paper, we consider the following analytical solution for the temperature

$$\mathrm{u}^{(\mathrm{an})}(\mathbf{x}) = \frac{1-\mathrm{e}^{-2(\beta_1 \mathrm{x}_1+\beta_2 \mathrm{x}_2)}}{1-\mathrm{e}^{-2(\beta_1+\beta_2)}}, \quad \mathbf{x} = (\mathrm{x}_1, \mathrm{x}_2) \in \overline{\Omega}, \tag{30}$$

whilst the corresponding analytical normal heat flux on the boundary $\partial\Omega$ is given by

$$\begin{aligned} \mathrm{q}^{(\mathrm{an})}(\mathbf{x}) &= \frac{-2}{1-\mathrm{e}^{-2(\beta_1+\beta_2)}} \left[\left(\mathrm{K}_{11}\beta_1+\mathrm{K}_{12}\beta_2\right) \mathrm{n}_1(\mathbf{x}) + \left(\mathrm{K}_{21}\beta_1+\mathrm{K}_{22}\beta_2\right) \mathrm{n}_2(\mathbf{x})\right], \\ \mathbf{x} &= (\mathrm{x}_1, \mathrm{x}_2) \in \partial\Omega. \end{aligned} \tag{31}$$

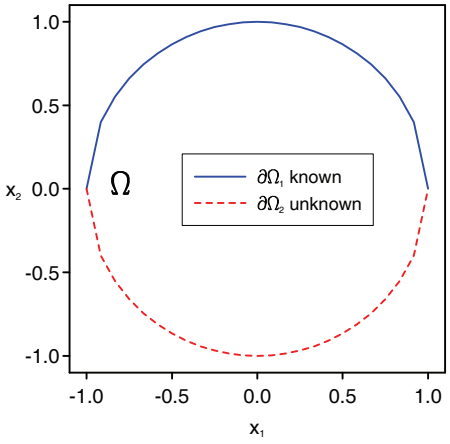

(a) Example 1: Disk

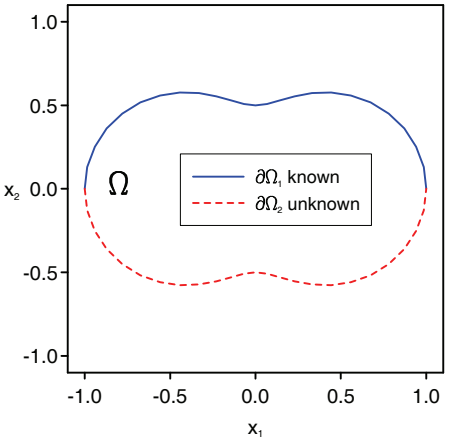

(b) Example 2: Peanut-shaped domain

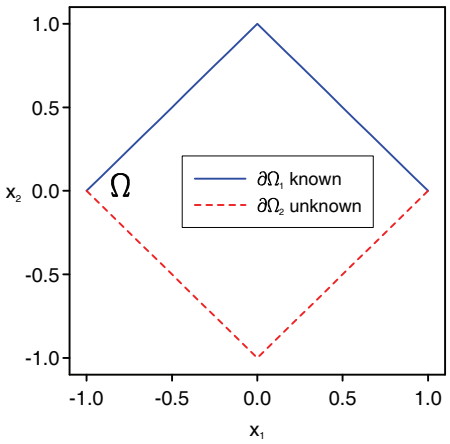

(c) Example 3: Rotated square

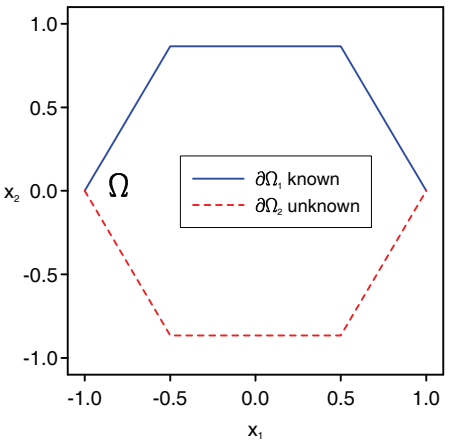

(d) Example 4: Hexagon

Figure 2: Schematic diagram of the domain Ω, and the known and unknown boundaries $\partial\Omega_1$ and $\partial\Omega_2$, respectively, for the inverse geometric problems analyzed.

Example 1. We consider the unit disk $\Omega = \left\{\mathbf{x} = (x_1, x_2) \middle| x_1^2 + x_2^2 < r^2\right\}$, $r = 1.0$, whose boundary $\partial\Omega$ consists of two parts, namely

$$\partial\Omega_1 = \left\{\mathbf{x} = (x_1, x_2) \middle| -1 \leq x_1 \leq 1; x_2 = \sqrt{r^2 - x_1^2}\right\} \tag{32a}$$

and

$$\partial\Omega_2 = \left\{ \mathbf{x} = (x_1, x_2) \,\middle|\, -1 < x_1 < 1;\, x_2 = -\sqrt{r^2 - x_1^2} \right\}. \tag{32b}$$

Example 2. We consider the peanut-shaped domain $\Omega = \left\{ \mathbf{x} = (x_1, x_2) \middle| x_1^2 + x_2^2 < r^2(\theta);\, \theta \in [0, 2\pi) \right\}$, where $r^2(\theta) = \cos^2(\theta) + \frac{1}{4}\sin^2(\theta)$, which is bounded by the following curves

$$\partial\Omega_1 = \left\{ \mathbf{x} = (x_1, x_2) \middle| x_1 = r(\theta)\cos(\theta);\, x_2 = r(\theta)\sin(\theta);\, \theta \in [0, \pi] \right\} \tag{33a}$$

and

$$\partial\Omega_2 = \left\{ \mathbf{x} = (x_1, x_2) \middle| x_1 = r(\theta)\cos(\theta);\, x_2 = r(\theta)\sin(\theta);\, \theta \in (\pi, 2\pi) \right\}. \tag{33b}$$

Example 3. We consider the domain Ω as the square $\left(-r/\sqrt{2}, r/\sqrt{2}\right)^2$, $r = 1.0$, rotated by an angle $\theta = \pi/4$, whose boundary $\partial\Omega$ consists of two parts, namely

$$\begin{aligned} \partial\Omega_1 \;&= \left\{ \mathbf{x} = (x_1, x_2) \middle| 0 \le x_1 \le r;\, x_2 = r - x_1 \right\} \\ &\cup \left\{ \mathbf{x} = (x_1, x_2) \middle| -r \le x_1 \le 0;\, x_2 = r + x_1 \right\} \end{aligned} \tag{34a}$$

and

$$\begin{aligned} \partial\Omega_2 \;&= \left\{ \mathbf{x} = (x_1, x_2) \middle| -r < x_1 \le 0;\, x_2 = -(r + x_1) \right\} \\ &\cup \left\{ \mathbf{x} = (x_1, x_2) \middle| 0 \le x_1 < r;\, x_2 = -(r - x_1) \right\}. \end{aligned} \tag{34b}$$

Example 4. We consider the hexagonal domain Ω inscribed in the circle $\partial B(0; r) = \left\{ \mathbf{x} = (x_1, x_2) \middle| x_1^2 + x_2^2 = r^2 \right\}$, $r = 1.0$, which is bounded by the following curves

$$\begin{aligned} \partial\Omega_1 \;&= \left\{ \mathbf{x} = (x_1, x_2) \,\middle|\, \frac{r}{2} < x_1 \le r;\, x_2 = (r - x_1)\sqrt{3} \right\} \\ &\cup \left\{ \mathbf{x} = (x_1, x_2) \,\middle|\, -\frac{r}{2} \le x_1 \le -\frac{r}{2};\, x_2 = r\frac{\sqrt{3}}{2} \right\} \\ &\cup \left\{ \mathbf{x} = (x_1, x_2) \,\middle|\, -r \le x_1 < -\frac{r}{2};\, x_2 = (r + x_1)\sqrt{3} \right\} \end{aligned} \tag{35a}$$

and

$$\begin{aligned}\partial\Omega_2 &= \left\{\mathbf{x}=(\mathrm{x}_1,\mathrm{x}_2)\,\middle|\,-\mathrm{r}<\mathrm{x}_1<\frac{\mathrm{r}}{2};\,\mathrm{x}_2=-(\mathrm{r}+\mathrm{x}_1)\sqrt{3}\right\}\\ &\cup\left\{\mathbf{x}=(\mathrm{x}_1,\mathrm{x}_2)\,\middle|\,-\frac{\mathrm{r}}{2}\le\mathrm{x}_1\le\frac{\mathrm{r}}{2};\,\mathrm{x}_2=-\mathrm{r}\frac{\sqrt{3}}{2}\right\}\\ &\cup\left\{\mathbf{x}=(\mathrm{x}_1,\mathrm{x}_2)\,\middle|\,\frac{\mathrm{r}}{2}<\mathrm{x}_1<\mathrm{r};\,\mathrm{x}_2=-(\mathrm{r}-\mathrm{x}_1)\sqrt{3}\right\}.\end{aligned}\tag{35b}$$

The inverse geometric problems investigated in this paper have been solved using the uniform distribution of both the MFS boundary collocation points $\mathbf{x}^{(i)}$, $i=1,\ldots,N$, and the singularities $\boldsymbol{\xi}^{(j)}$, $j=1,\ldots,M$, as described in Sections 3.1 and 3.3, respectively. Furthermore, the numbers of MFS boundary collocation points N_1 and N_2 corresponding to the known $\partial\Omega_1$ and unknown $\partial\Omega_2$ boundaries, respectively, as well as the radius of the disk on whose boundary the singularities are situated, were set to:

(*i*) $N_1=N_2=12$ and $\mathrm{R}_S=2.0$ for Examples 1, 3 and 4;

(*ii*) $N_1=N_2=10$ and $\mathrm{R}_S=3.0$ for Example 2.

In addition, for Examples $1-4$ the number of singularities was taken to be equal to that of MFS boundary collocation points, i.e. $M=N=N_1+N_2$. Also, for all examples investigated in this paper, the Tikhonov first-order regularization functional (17) has been minimized subject to the physical constraints (22), see also Eq. (23), and this is consistent with the shape of the unknown boundary $\partial\Omega_2$ considered in Examples $1-4$, see Eqs. (32*b*), (33*b*), (34*b*) and (35*b*). Moreover, in all examples, the initial guesses for the unknown MFS coefficients $\mathbf{c}=[\mathrm{c}_1,\ldots,\mathrm{c}_M]^{\mathsf{T}}$ and the unknown x_2-coordinates $\mathbf{z}=\left[\mathrm{z}_2^{(N_1+2)},\ldots,\mathrm{z}_2^{(N_1+N_2)}\right]^{\mathsf{T}}$ of the boundary points that determine the unknown boundary $\partial\Omega_2$ were taken as:

(*i*) $\eta_\ell=\mathrm{c}_\ell=1.0\times10^{0}$, $\ell=1,\ldots,M$;

(*ii*) $\eta_{M+\ell}=\mathrm{z}_2^{(N_1+\ell+1)}=-1.0\times10^{-15}$, $\ell=1,\ldots,N_2-1$.

5.2 Numerical results obtained without regularization

In what follows, the temperature, $\mathrm{u}|_{\partial\Omega_1}=\mathrm{u}^{(\mathrm{an})}|_{\partial\Omega_1}$, and/or the normal heat flux, $\mathrm{q}|_{\partial\Omega_1}=\mathrm{q}^{(\mathrm{an})}|_{\partial\Omega_1}$, on the known boundary have been perturbed as

$$\widetilde{\mathrm{u}}^{\epsilon}|_{\partial\Omega_1}=\mathrm{u}|_{\partial\Omega_1}+\delta\mathrm{u},\quad \delta\mathrm{u}=\texttt{G05DDF}(0,\sigma_1),\quad \sigma_1=\max_{\partial\Omega_1}|\mathrm{u}|\times(p_1/100),\tag{36}$$

and

$$\widetilde{\mathrm{q}}^{\epsilon}|_{\partial\Omega_1} = \mathrm{q}|_{\partial\Omega_1} + \delta\mathrm{q}, \quad \delta\mathrm{q} = \texttt{G05DDF}(0,\sigma_2), \quad \sigma_2 = \max_{\partial\Omega_1}|\mathrm{q}| \times (p_2/100), \tag{37}$$

respectively. Here δu and δq are Gaussian random variables with mean zero and standard deviations σ_1 and σ_2, respectively, generated by the NAG subroutine G05DDF [NAG Library Mark 21 (2007)], while $p_1\%$ and $p_2\%$ are the percentages of additive noise included into the input boundary temperature, $\mathrm{u}|_{\partial\Omega_1}$, and normal heat flux, $\mathrm{q}|_{\partial\Omega_1}$, respectively, in order to simulate the inherent measurement errors.

The initial guess, exact and reconstructed values for the boundary $\partial\Omega_2$, obtained in the case of Example 2 using the least-squares functional (18) subject to the physical constraints (22), perturbed Dirichlet data and exact Neumann data on $\partial\Omega_1$ and exact Dirichlet data on $\partial\Omega_2$, and exact Dirichlet data and perturbed Neumann data on $\partial\Omega_1$ and exact Neumann data on $\partial\Omega_2$, are illustrated in Figs. 3(a) and 3(b), respectively. As can be observed from these figures, the MFS approximations are not only poor, but also highly oscillatory and, in some cases unbounded, i.e. unstable. At the same time, Figs. 3(a) and 3(b) clearly show the necessity of employing regularization methods to obtain accurate and stable solutions to the inverse geometric problems investigated. Similar results have been obtained for the other examples analyzed in this paper and, therefore, they are not illustrated.

5.3 Accuracy errors

In order to analyze the accuracy of the numerical results obtained for the unknown boundary, $\partial\Omega_2$, of the two-dimensional domain, Ω, occupied by an FGM, using various values of the regularization parameter, $\lambda > 0$, we define the *root mean-square* (*RMS*) *error* by

$$\mathrm{e}_{\mathbf{z}}(\lambda) = \sqrt{\frac{1}{N_2-1}\sum_{i=N_1+2}^{N_1+N_2}\left(\mathrm{z}_2^{(i;\lambda)} - \mathrm{z}_2^{(i;\mathrm{an})}\right)^2}, \quad \lambda > 0, \tag{38}$$

where $\mathrm{z}_2^{(i;\lambda)}$ is the numerically retrieved value corresponding to the regularization parameter, $\lambda > 0$, for the exact x_2-coordinate, $\mathrm{z}_2^{(i;\mathrm{an})}$, that determines the unknown boundary, $\partial\Omega_2$.

Figs. 4(a) and 4(b) present on a log-log scale the RMS error, $\mathrm{e}_{\mathbf{z}}$, defined by Eq. (38), as a function of the regularization parameter, λ, obtained using perturbed Dirichlet data on the known boundary, $\partial\Omega_1$, exact Dirichlet data on the unknown

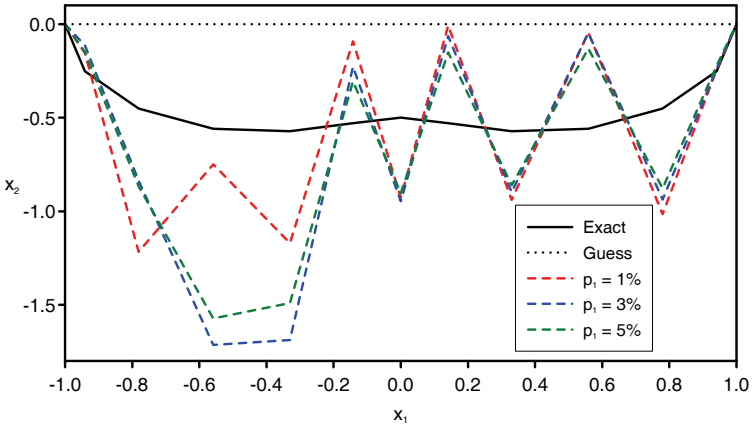

(a) Perturbed Dirichlet data on $\partial\Omega_1$ and exact Dirichlet data on $\partial\Omega_2$

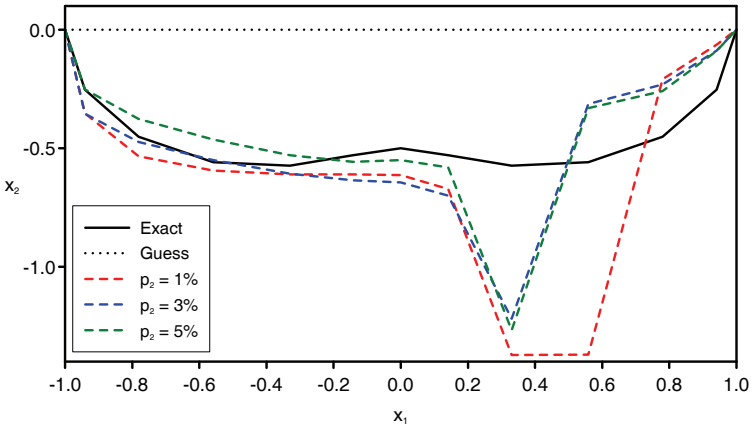

(b) Perturbed Neumann data on $\partial\Omega_1$ and exact Neumann data on $\partial\Omega_2$

Figure 3: Initial guess, exact and reconstructed values for the boundary $\partial\Omega_2$, obtained with perturbed Cauchy data on $\partial\Omega_1$, exact (a) Dirichlet, and (b) Neumann data on $\partial\Omega_2$, and the least-squares method, in the case of Example 2.

boundary, $\partial\Omega_2$, and the MFS-based Tikhonov first-order regularization method described in Section 4, for the inverse geometric problems given by Examples 1 and 2, respectively. From these figures it can be seen that the minimum value of the RMS error decreases as the level of noise added into the Dirichlet data on $\partial\Omega_1$ increases, therefore emphasizing the numerical stability of the proposed method.

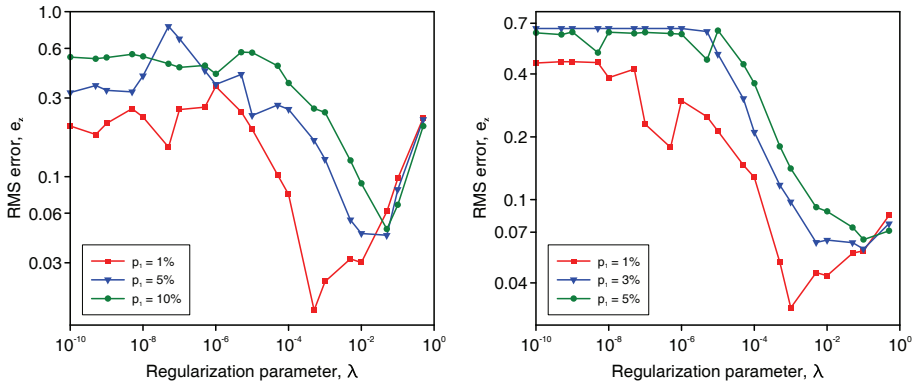

(a) Example 1 (b) Example 2

Figure 4: The RMS error, $e_{\mathbf{z}}$, as a function of the regularization parameter, λ, obtained with perturbed Dirichlet data on $\partial\Omega_1$, exact Dirichlet on $\partial\Omega_2$ and the Tikhonov regularization method, for (a) Example 1, and (b) Example 2.

5.4 Selection of the optimal regularization parameter

The performance of regularization methods depends crucially on the suitable choice of the regularization parameter. One extensively studied criterion is the discrepancy principle, see e.g. Morozov (1966). Although this criterion is mathematically rigorous, it requires a reliable estimation of the amount of noise added into the data which may not be available in practical problems. Heuristical approaches are preferable in the case when no *a priori* information about the noise is available. Several heuristical approaches have been proposed for the Tikhonov regularization method, including the L-curve criterion, see Hansen (1998), and the generalized cross-validation, see Wahba (1977). In this paper, we employ the L-curve criterion to determine the optimal regularization parameter, λ_{opt}, for the proposed numerical method.

If we define on a logarithmic scale the following curve

$$\left\{ \left(\sqrt{2\mathscr{F}_{LS}(\boldsymbol{\eta}_\lambda)}, \sqrt{2\mathscr{R}(\mathbf{z}_\lambda)} \right) \,\middle|\, \lambda > 0 \right\} = \left\{ \left(\|\mathbf{F}(\boldsymbol{\eta}_\lambda) - \mathbf{y}\|, \|\mathbf{z}_\lambda\| \right) \,\middle|\, \lambda > 0 \right\}, \tag{39}$$

where $\mathbf{F}(\boldsymbol{\eta}) = \left[\overline{\mathrm{F}}_1(\boldsymbol{\eta}), \ldots, \overline{\mathrm{F}}_{N_1+N_2}(\boldsymbol{\eta})\right]^{\mathsf{T}}$ and $\mathbf{y} = \left[\overline{\mathrm{y}}_1, \ldots, \overline{\mathrm{y}}_{N_1+N_2}\right]^{\mathsf{T}}$, then this typically has an L-shaped form and hence it is referred to as the L-curve. According to the L-curve criterion, the optimal regularization parameter corresponds to the corner of the L-curve since a good tradeoff between the residual and solution norms is achieved at this point. Numerically, the L-curve method is robust and stable with

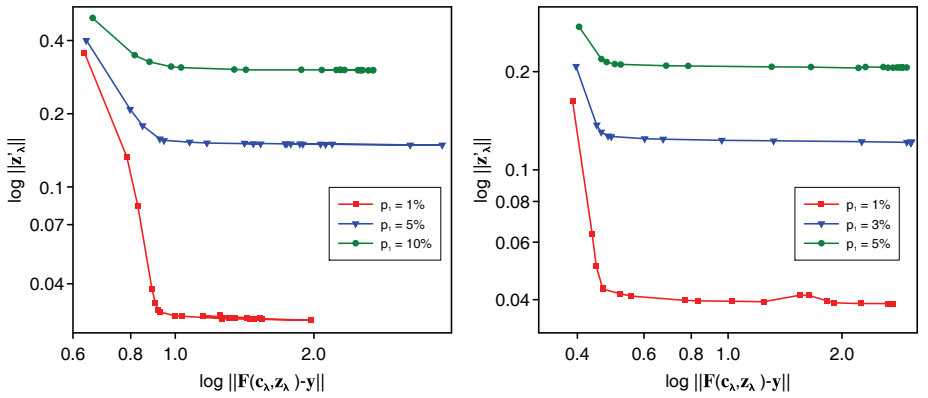

(a) Example 1 (b) Example 2

Figure 5: The L-curves obtained with perturbed Dirichlet data on $\partial\Omega_1$, exact Dirichlet on $\partial\Omega_2$ and the Tikhonov regularization method, in the case of (a) Example 1, and (b) Example 2.

respect to both uncorrelated and highly correlated noise. Furthermore, this criterion works effectively with certain classes of practical problems, see Hansen (1998) and Chen, Chen, Hong and Chen (1995). For a discussion of the theoretical aspects of the L-curve criterion, we refer the reader to Hanke (1996) and Vogel (1996).

Figs. $5(a)$ and $5(b)$ illustrate clearly the L-shaped curves retrieved using perturbed Dirichlet data and exact Neumann data on the known boundary, $\partial\Omega_1$, exact Dirichlet on the unknown boundary, $\partial\Omega_2$ and the Tikhonov regularization method, in the case of Examples 1 and 2, respectively; therefore, Hansen's L-curve criterion is applicable. The corresponding values for the optimal regularization parameter, λ_{opt}, obtained according to the aforementioned criterion, are as follows:

(*i*) $\lambda_{\text{opt}} = 5.0 \times 10^{-4}$ and $\lambda_{\text{opt}} = 5.0 \times 10^{-2}$ for $p_1 = 1\%$, and $p_1 = 5\%, 10\%$, respectively, in the case of Example 1;

(*ii*) $\lambda_{\text{opt}} = 1.0 \times 10^{-3}$ and $\lambda_{\text{opt}} = 1.0 \times 10^{-1}$ for $p_1 = 1\%$ and $p_1 = 3\%, 5\%$, respectively, in the case of Example 2.

On comparing Figs. 4 and 5, it can be seen that, for both Examples 1 and 2 and all levels of noise added into the Dirichlet data on $\partial\Omega_1$, the minimum in the RMS accuracy error, $e_{\mathbf{z}}$, is attained for $\lambda \approx \lambda_{\text{opt}}$, with λ_{opt} given by the L-curve criterion. Similar results have been obtained for the other inverse geometric problems investigated in this study and hence they are not presented here. Therefore, we can

conclude that Hansen's L-curve criterion provides very good approximations for the optimal regularization parameter.

5.5 Numerical results obtained with regularization

Figs. $6(a)$ and $6(b)$ show the initial guess, the exact and numerical values for the unknown boundary, $\partial\Omega_2$, obtained using the regularized MFS algorithm described in Section 4, the optimal regularization parameter, $\lambda = \lambda_{\text{opt}}$, chosen according to the L-curve criterion, and various levels of noise added into the temperature data $\mathrm{u}|_{\partial\Omega_1}$ for the inverse geometric problem $(6a)-(6d)$ with $\alpha_{\mathrm{u}} = 1$ and $\alpha_{\mathrm{q}} = 0$, and the normal heat flux data $\mathrm{q}|_{\partial\Omega_1}$ for the inverse geometric problem $(6a)-(6d)$ with $\alpha_{\mathrm{u}} = 0$ and $\alpha_{\mathrm{q}} = 1$, respectively, in the case of Example 1. From these figures, it can be observed that for Example 1 the numerical solutions are stable and consistent with respect to the amounts of noise p_1 and p_2 added into the input Dirichlet and Neumann data, respectively, on the accessible boundary $\partial\Omega_1$. Moreover, for both inverse problems associated with Example 1, the numerically retrieved solutions converge to their corresponding exact solution given by Eq. $(32b)$.

The MFS-based Tikhonov first-order regularization method presented in Section 4, in conjunction with Hansen's L-curve criterion for determining the optimal value of the regularization parameter, produces stable and consistent numerical solutions with respect to the amount of noise added into the Dirichlet or Neumann data on the known part of the boundary, $\partial\Omega_1$, which are at the same time accurate approximations for and convergent towards their corresponding exact value, also in the case of two-dimensional non-convex domains with a smooth boundary, such as the peanut-shaped domain occupied by an FGM and considered in Example 2, see Eq. (33). These results can be observed from Figs. $7(a)$ and $7(b)$ which illustrate the initial guess, the exact and numerically retrieved values for the unknown boundary given by Eq. $(33b)$, for perturbed Dirichlet ($p_1 = 1\%, 3\%$ and 5%) and exact Neumann data on $\partial\Omega_1$ and exact Dirichlet data on $\partial\Omega_2$, and exact Dirichlet and noisy Neumann data ($p_2 = 1\%, 3\%$ and 5%) on $\partial\Omega_1$ and exact Neumann data on $\partial\Omega_2$, respectively.

The proposed MFS-Tikhonov regularization procedure works equally well also for the inverse geometric problem $(6a)-(6d)$ in two-dimensional domains occupied by an FGM and bounded by a piecewise smooth boundary, such as the rotated square and the hexagonal domain considered in Examples 3 and 4, respectively, with perturbed Cauchy data on the accessible part of the boundary, $\partial\Omega_1$, i.e. $p_1 > 0$ and/or $p_2 > 0$, and either exact Dirichlet ($\alpha_{\mathrm{u}} = 1$ and $\alpha_{\mathrm{q}} = 0$) or Neumann ($\alpha_{\mathrm{u}} = 0$ and $\alpha_{\mathrm{q}} = 1$) data on the unknown boundary, $\partial\Omega_2$. The initial guess, the exact and numerical values for the unknown boundary, $\partial\Omega_2$, in the case of Examples 3 and 4, obtained using the regularization method presented in Section 4, the optimal regu-

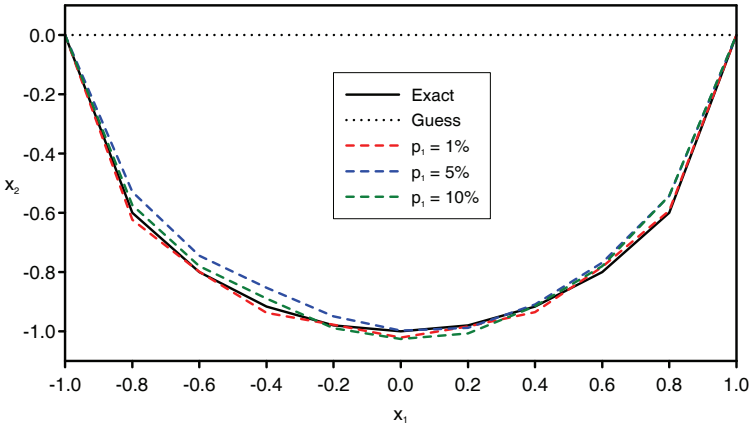

(a) Perturbed Dirichlet data on $\partial\Omega_1$ and exact Dirichlet data on $\partial\Omega_2$

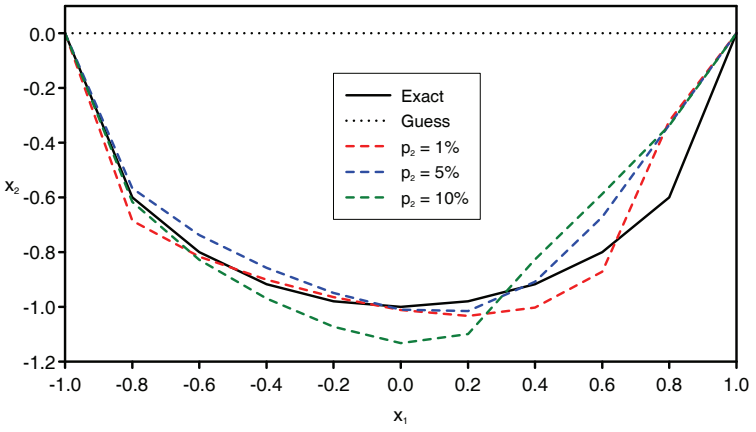

(b) Perturbed Neumann data on $\partial\Omega_1$ and exact Neumann data on $\partial\Omega_2$

Figure 6: Initial guess, exact and reconstructed values for the boundary $\partial\Omega_2$, obtained with perturbed Cauchy data on $\partial\Omega_1$, exact (a) Dirichlet, and (b) Neumann data on $\partial\Omega_2$, and the Tikhonov regularization method, in the case of Example 1.

larization parameter, $\lambda = \lambda_{\text{opt}}$, selected by Hansen's L-curve criterion, and various levels of noise added into the Cauchy data, are shown in Figs. 8 and 9, respectively. However, it can be noted from these figures that, in both Examples 3 and 4, the corner points are, as expected, slightly rounded-off since the minimization of the Tikhonov first-order regularization functional (17) subject to the physical constraints (22) imposes the numerical solution to be smooth.

Although not illustrated herein, it is reported that accurate, convergent, consistent

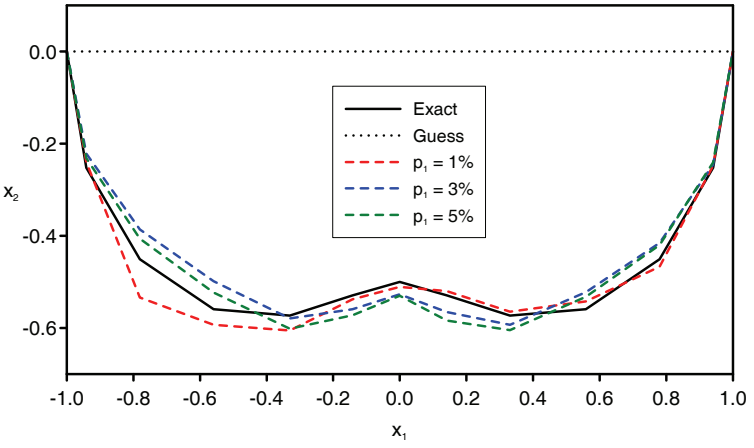

(a) Perturbed Dirichlet data on $\partial\Omega_1$ and exact Dirichlet data on $\partial\Omega_2$

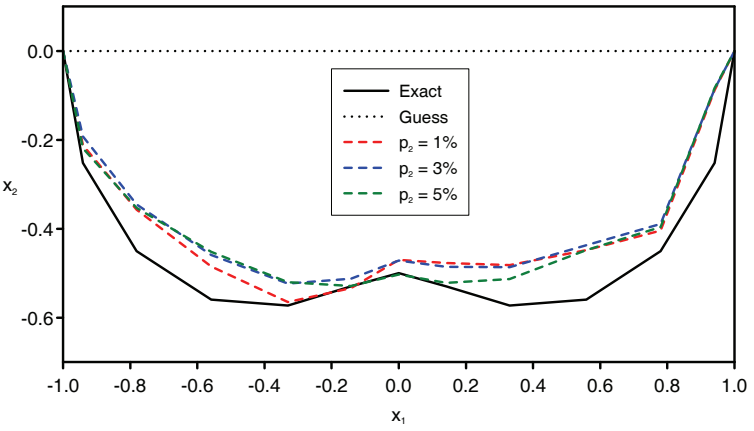

(b) Perturbed Neumann data on $\partial\Omega_1$ and exact Neumann data on $\partial\Omega_2$

Figure 7: Initial guess, exact and reconstructed values for the boundary $\partial\Omega_2$, obtained with perturbed Cauchy data on $\partial\Omega_1$, exact (a) Dirichlet, and (b) Neumann data on $\partial\Omega_2$, and the Tikhonov regularization method, in the case of Example 2.

and stable numerical approximations for the inaccessible boundary, $\partial\Omega_2$, have also been obtained for the inverse problem $(6a)-(6d)$ in a convex or non-convex domain occupied by an FGM material and bounded by a smooth or piecewise smooth boundary, with noisy Cauchy data on the accessible part of the boundary, $\partial\Omega_1$, and exact Robin condition ($\alpha_u\,\alpha_q \neq 0$) on the inaccessible boundary, $\partial\Omega_2$. It is also important to mention that taking $R_S \geq 1.50$ does not affect significantly the errors of the numerical results obtained for all examples investigated in this study.

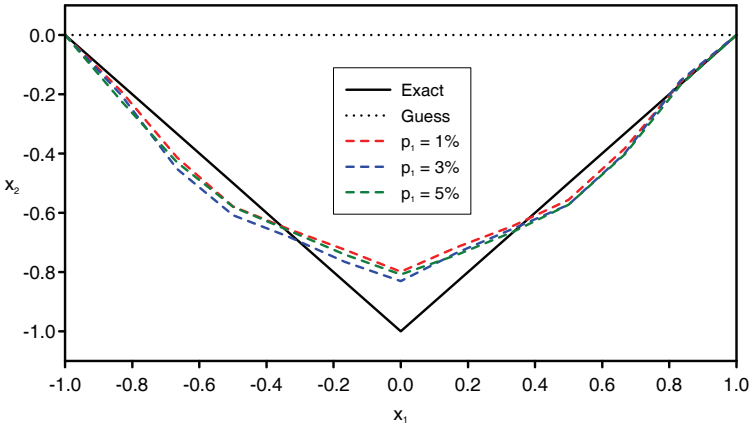

(a) Perturbed Dirichlet data on $\partial\Omega_1$ and exact Dirichlet data on $\partial\Omega_2$

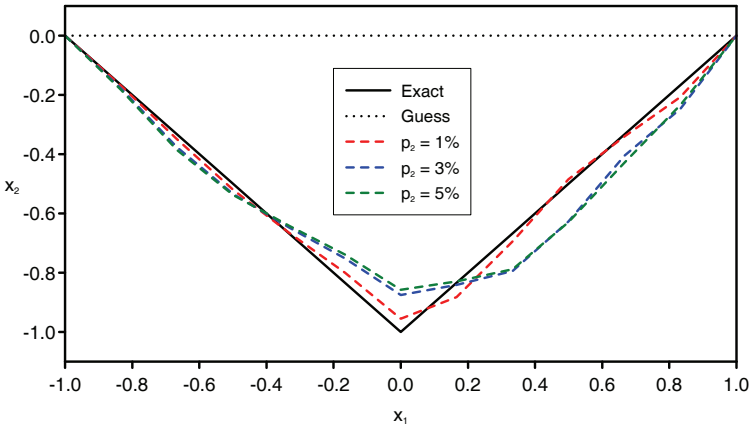

(b) Perturbed Neumann data on $\partial\Omega_1$ and exact Neumann data on $\partial\Omega_2$

Figure 8: Initial guess, exact and reconstructed values for the boundary $\partial\Omega_2$, obtained with perturbed Cauchy data on $\partial\Omega_1$, exact (a) Dirichlet, and (b) Neumann data on $\partial\Omega_2$, and the Tikhonov regularization method, in the case of Example 3.

6 Conclusions

The MFS was applied for solving accurately and stably an inverse problem associated with two-dimensional FGMs, namely the detection of an unknown portion of the boundary from a given exact boundary condition on this part of the boundary and additional noisy Dirichlet and Neumann data (i.e. Cauchy data) on the remaining known portion of the boundary. This inverse geometric problem is ill-posed and recasts in discrete form as an ill-conditioned system of nonlinear algebraic equa-

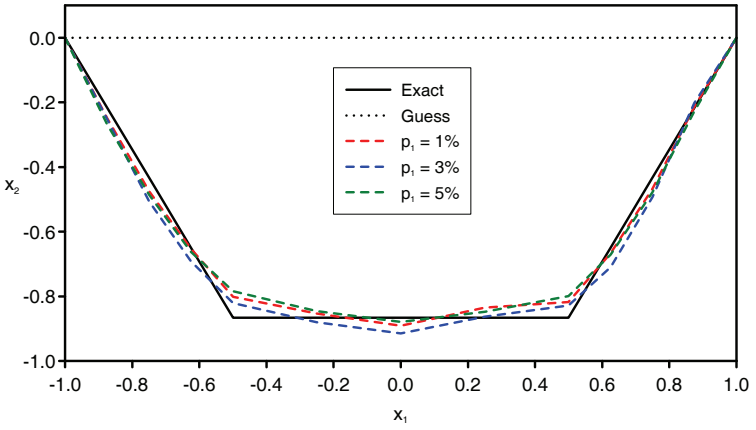

(a) Perturbed Dirichlet data on $\partial\Omega_1$ and exact Dirichlet data on $\partial\Omega_2$

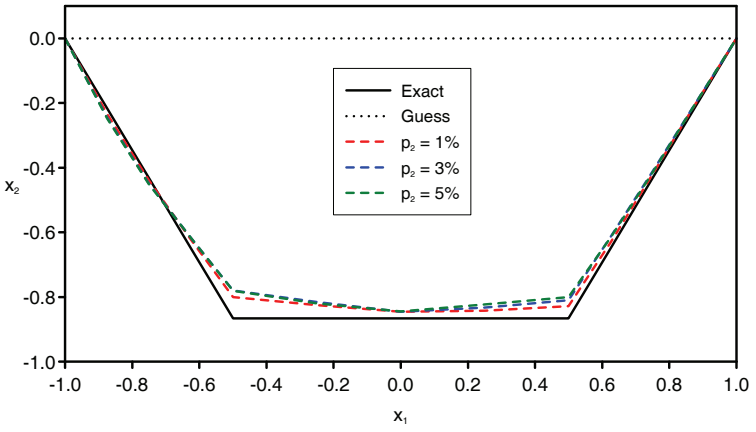

(b) Perturbed Neumann data on $\partial\Omega_1$ and exact Neumann data on $\partial\Omega_2$

Figure 9: Initial guess, exact and reconstructed values for the boundary $\partial\Omega_2$, obtained with perturbed Cauchy data on $\partial\Omega_1$, exact (a) Dirichlet, and (b) Neumann data on $\partial\Omega_2$, and the Tikhonov regularization method, in the case of Example 4.

tions, which was solved in a stable manner by using the Tikhonov first-order regularization method. The optimal value of the regularization parameter was chosen according to Hansen's L-curve criterion. Various examples for two-dimensional simply connected, convex and non-convex domains occupied by an FGM and having smooth and piecewise smooth boundaries, were considered. From the numerical results presented in this study it can be concluded that the proposed method is consistent and stable with respect to decreasing the amount of noise added into the

Cauchy data, accurate and computationally very efficient.

The present method can be extended to other two-dimensional inverse geometric problems associated with partial differential operators whose fundamental solutions are available, such as the Lamé system of linear elasticity, Helmholtz-type equations and anisotropic heat conduction, as well as similar three-dimensional inverse geometric problems, but these are deferred as future work.

Acknowledgement: The financial support received from the Romanian Ministry of Education, Research and Innovation through IDEI Programme, Exploratory Research Projects, Grant PN II–ID–PCE–1248/2008, is gratefully acknowledged.

References

Ahmadabadi, M. N.; Arab, M.; Ghaini, F. M. M. (2009): The method of fundamental solutions for the inverse space-dependent heat source problem. *Engineering Analysis with Boundary Elements*, vol. 33, pp. 1231–1235.

Chen, L. Y.; Chen, J. T.; Hong, H. K.; Chen, C. H. (1995): Application of Cesàro mean and the L-curve for the dconvolution problem. *Soil Dynamics Earthquake Engineering*, vol. 14, pp. 361–373.

Chen, C. W.; Young, D. L.; Tsai, C. C.; Murugesan, K. (2005): The method of fundamental solutions for inverse 2D Stokes problems. *Computational Mechanics*, vol. 37, pp. 2–14.

Cho, H. A.; Golberg, M. A.; Muleshkov, A. S.; Li, X. (2004): Trefftz methods for time dependent partial differential equations. *CMC: Computers, Materials & Continua*, vol. 1, pp. 1–37.

Dong, C. F.; Sun, F. Y.; Meng, B. Q. (2007): A method of fundamental solutions for inverse heat conduction problems in an anisotropic medium. *Engineering Analysis with Boundary Elements*, vol. 31, pp. 75–82.

Engl, H. W.; Hanke, M.; Neubauer, A. (2000): *Regularization of Inverse Problems*. Kluwer Academic, Dordrecht.

Fairweather, G.; Karageorghis, A. (1998): The method of fundamental solutions for elliptic boundary value problems. *Advances in Computational Mathematics*, vol. 9, pp. 69–95.

Fairweather, G.; Karageorghis, A.; Martin, P. A. (2003): The method of fundamental solutions for scattering and radiation problems. *Engineering Analysis with Boundary Elements*, **27**, pp. 759–769.

Fam, G. S. A.; Rashed, Y. F. (2009): The method of fundamental solutions applied to 3D elasticity problems using a continuous collocation scheme. *Engineering Analysis with Boundary Elements*, vol. 33, pp. 330–341.

Gill, P. E.; Murray, W.; Wright, M. H. (1981): *Practical Optimization*. Academic Press, London.

Golberg, M. A.; Chen, C. S. (1999): The method of fundamental solutions for potential, Helmholtz and diffusion problems. In: M. A. Golberg (ed.) *Boundary Integral Methods: Numerical and Mathematical Aspects*, WIT Press and Computational Mechanics Publications, Boston, pp. 105–176.

Hadamard, J. (1923): *Lectures on Cauchy Problem in Linear Partial Differential Equations*. Yale University Press, New Haven.

Hanke, M. (1996): Limitations of the L-curve method in ill-posed problems. *BIT*, vol. 36, pp. 287–301.

Hansen, P. C. (1998): *Rank-Deficient and Discrete Ill-Posed Problems: Numerical Aspects of Linear Inversion*. SIAM, Philadelphia.

Hon, Y. C.; Li, M. (2008): A computational method for inverse free boundary determination problem. *International Journal for Numerical Methods in Engineering*, vol. 73, 1291–1309.

Hon, Y. C.; Wei, T. (2004): A fundamental solution method for inverse heat conduction problems. *Engineering Analysis with Boundary Elements*, vol. 28, pp. 489–495.

Hon, Y. C.; Wei, T. (2005): The method of fundamental solutions for solving multidimensional heat conduction problems. *CMES: Computer Modeling in Engineering & Sciences*, vol. 13, pp. 219–228.

Hon, Y. C.; Wu, Z. (2000): A numerical computation for inverse boundary determination problem. *Engineering Analysis with Boundary Elements*, vol. 24, 599–606.

Hsieh, C. K.; Kassab, A. J. (1986): A general method for the solution of inverse heat conduction problem with partially unknown system geometries. *International Journal of Heat and Mass Transfer*, vol. 29, 47–58.

Huang, C. C.; Kassab, B. H. (1997): An inverse geometry problem for identifying irregular boundary configurations. *International Journal of Heat and Mass Transfer*, vol. 40, 2045–2053.

Huang, C. C.; Tsai, C. C. (1997): A transient inverse two-dimensional geometry problem in estimating time-dependent irregular boundary configurations. *International Journal of Heat and Mass Transfer*, vol. 41, 1707–1718.

Jin, B. T.; Marin, L. (2007): The method of fundamental solutions for inverse source problems associated with the steady-state heat conduction. *International Journal for Numerical Methods in Engineering*, vol. 69, pp. 1570–1589.

Jin, B. T.; Zheng, Y. (2006): A meshless method for some inverse problems associated with the Helmholtz equation. *Computer Methods in Applied Mechanics and Engineering*, vol. 195, pp. 2270–2280.

Kunisch, K.; Zou, J. (1998): Iterative choices of regularization parameters in linear inverse problems. *Inverse Problems*, vol. 14, pp. 1247–1264.

Lesnic, D.; Berger, J. R.; Martin, P. A. (2002): A boundary element regularization method for the boundary determination in potential corrosion damage. *Inverse Problems in Engineering*, vol. 10, pp. 163–182.

Ling, L.; Takeuchi, T. (2008): Boundary control for inverse Cauchy problems of the Laplace equations. *CMES: Computer Modeling in Engineering & Sciences*, vol. 29, pp. 45–54.

Liu, C.–S. (2008a): Solving an inverse Sturm-Liouville problem by a Lie-group method. *Boundary Value Problems*, vol. 2008, Article ID 749865.

Liu, C.–S. (2008b): Identifying time-dependent damping and stiffness functions by a simple and yet accurate method. *Journal of Sound and Vibration*, vol. 318, pp. 148–165.

Liu, C.–S. (2008c): A Lie-group shooting method for simultaneously estimating the time-dependent damping and stiffness coefficients. *CMES: Computer Modeling in Engineering & Sciences*, vol. 27, pp. 137–149.

Liu, C.–S. (2008d): A time-marching algorithm for solving non-linear obstacle problems with the aid of an NCP-function. *CMC: Computers, Materials & Continua*, vol. 8, pp. 53–65.

Liu, C.–S. (2008e): A fictitious time integration method for two-dimensional quasilinear elliptic boundary value problems. *CMES: Computer Modeling in Engineering & Sciences*, vol. 33, pp. 179–198.

Liu, C.–S. (2008f): A fictitious time integration method for solving m-point boundary value problems. *CMES: Computer Modeling in Engineering & Sciences*, vol. 39, pp. 125–154.

Liu, C.–S.; Atluri, S. N. (2008a): A fictitious time integration method (FTIM) for solving mixed complementarity problems with applications to non-linear optimization. *CMES: Computer Modeling in Engineering & Sciences*, vol. 34, pp. 155–178.

Liu, C.–S.; Atluri, S. N. (2008b): A novel fictitious time integration method for solving the discretized inverse Sturm-Liouville problems, for specified eigenvalues. *CMES: Computer Modeling in Engineering & Sciences*, vol. 36, pp. 261–285.

Liu, C.–S.; Atluri, S. N. (2009): A fictitious time integration method for the numerical solution of the Fredholm integral equation and for numerical differentiation of noisy data, and its relation with the filter theory. *CMES: Computer Modeling in Engineering & Sciences*, vol. 41, pp. 243–261.

Liu, C.–S.; Chang, J. R.; Chang, K. H.; Chen, Y. W. (2008): Simultaneously estimating the time-dependent damping and stiffness coefficients with the aid of vibrational data. *CMC: Computers, Materials & Continua*, vol. 7, pp. 97–107.

Marin, L. (2005a): A meshless method for solving the Cauchy problem in three-dimensional elastostatics. *Computers and Mathematics with Applications*, vol. 50, pp. 73–92.

Marin, L. (2005b): Numerical solutions of the Cauchy problem for steady-state heat transfer in two-dimensional functionally graded materials. *International Journal of Solids and Structures*, vol. 42, pp. 4338–4351.

Marin, L. (2005c): A meshless method for the numerical solution of the Cauchy problem associated with three-dimensional Helmholtz-type equations. *Applied Mathematics and Computation*, vol. 165, pp. 355–374.

Marin, L. (2006): Numerical boundary identification for Helmholtz-type equations. *Computational Mechanics*, vol. 39, pp. 25–40.

Marin, L. (2008): The method of fundamental solutions for inverse problems associated with the steady-state heat conduction in the presence of sources. *CMES: Computer Modeling in Engineering & Sciences*, vol. 30, pp. 99–122.

Marin, L.; Lesnic, D. (2003): BEM first-order regularisation method in linear elasticity for boundary identification. *Computer Methods in Applied Mechanics and Engineering*, vol. 192, pp. 2059–2071.

Marin, L.; Lesnic, D. (2004): The method of fundamental solutions for the Cauchy problem in two-dimensional linear elasticity. *International Journal of Solids and Structures*, vol. 41, pp. 3425–3438.

Marin, L.; Lesnic, D. (2005a): The method of fundamental solutions for the Cauchy problem associated with two-dimensional Helmholtz-type equations. *Computers & Structures*, vol. 83, pp. 267–278.

Marin, L.; Lesnic, D. (2005b): The method of fundamental solutions for inverse boundary value problems associted with the two dimentional biharmonic equation. *Mathematical and Computers in Modelling*, vol. 42, pp. 261–278.

Marin, L.; Karageorghis, A.; Lesnic, D. (2009): The MFS for boundary identification in two-dimensional harmonic problems, submitted.

Mathon, R.; Johnston, R. L. (1977): The approximate solution of elliptic boundary value problems by fundamental solutions. *SIAM Journal on Numerical Analysis*, vol. 14, pp. 638–650.

Mera, N. S. (2005): The method of fundamental solutions for the backward heat conduction problem. *Inverse Problems in Science and Engineering*, vol. 13, pp. 79–98.

Mera, N. S.; Lesnic; D. (2005): A three-dimensional boundary determination problem in potential corrosion damage. *Computational Mechanics*, vol. 36, pp. 129–138.

Morozov, V. A. (1966): On the solution of functional equations by the method of regularization. *Doklady Mathematics*, vol. 7, pp. 414–417.

Numerical Algorithms Group Library Mark 21 (2007). NAG(UK) Ltd, Wilkinson House, Jordan Hill Road, Oxford, UK.

Park, H. M.; Ku, J. H. (2001): Shape identification for natural convection problems. *Communications in Numerical Methods in Engineering*, vol. 17, pp. 871–880.

Peneau, S.; Jarny, Y.; Sarda, A. (1966): Isotherm Shape Identification for a Two-Dimensional Heat Conduction Problem. In: H. D. Bui, M. Tanaka, M. Bonnet, H. Maigre, E. Luzzato and M. Reynier (eds.) *Inverse Problems in Engineering Mechanics*, Balkema, Rotterdam, pp. 47–53.

Shigeta, T.; Young, D. L. (2009): Method of fundamental solutions with optimal regularization techniques for the Cauchy problem of the Laplace equation with singular points. *Journal of Computational Physics*, vol. 228, pp. 1903–1915.

Suresh, S.; Mortensen, A. (1998): *Fundamentals of Functionally Graded Materials*. IOM Communications Ltd., London.

Tikhonov, A. N.; Arsenin, V. Y. (1986): *Methods for Solving Ill-Posed Problems*. Nauka, Moscow.

Vogel, C. R. (1996): Non-convergence of the L-curve regularization parameter selection method. *Inverse Problems*, vol. 12, pp. 535–547.

Wahba, G. (1977): Practical approximate solutions to linear operator equations when the data are noisy. *SIAM Journal on Numerical Analysis*, vol. 14, pp. 651–667.

Yan, L.; Fu, C.–L.; Yang, F.–L. (2008): The method of fundamental solutions for the inverse heat source problem. *Engineering Analysis with Boundary Elements*, vol. 32, pp. 216–222.

Young, D. L.; Tsai, C. C.; Chen, C. W.; Fan, C. M. (2008): The method of fundamental solutions and condition number analysis for inverse problems of Laplace equation. *Computers and Mathematics with Applications*, vol. 55, pp. 1189–1200.

Zeb, A.; Ingham, D. B.; Lesnic, D. (2008): The method of fundamental solutions for a biharmonic boundary determination, *Computational Mechanics*, vol. 42, pp. 371–379.